5-14-2020

Kinetics of pHLIP peptide insertion into and exit from a membrane

Gregory Slaybaugh

Dhammika Weerakkody

Donald M. Engleman

Oleg A. Andreev
University of Rhode Island, andreev@uri.edu

Yana Reshetnyak
University of Rhode Island, reshetnyak@uri.edu

Citation/Publisher Attribution

Gregory Slaybaugh, Dhammika Weerakkody, Donald M. Engelman, Oleg A. Andreev, Yana K. Reshetnyak. Kinetics of pHLIP peptide insertion into and exit from a membrane. Proceedings of the National Academy of Sciences Jun 2020, 117 (22) 12095-12100; DOI: 10.1073/pnas.1917857117

BIOLOGICAL SCIENCES: Biophysics and Computational Biology

Kinetics of pHLIP peptide insertion into and exit from a membrane

Gregory Slaybaugh[a], Dhammika Weerakkody[a],
Donald M. Engelman[b], Oleg A. Andreev[a], Yana K. Reshetnyak[a,1]

[a]Physics Department, University of Rhode Island, Kingston, RI 02881;

[b]Department of Molecular Biophysics and Biochemistry, Yale, New Haven, CT 06511

Corresponding Author

[1]To whom correspondence should be addressed, e-mail: reshetnyak@uri.edu

Keywords

membrane-associated folding, tumor acidity, kinetics, fluorescence, pHLIP

Author Contributions

O.A.A., D.M.E and Y.K.R. designed research; G.S. and D.W. performed experiments; G.S. and Y.K.R. analyzed data; D.M.E., O.A.A. and Y.K.R. wrote the paper.

Conflict of Interest Statement

D.M.E., O.A.A. and Y.K.R. are founders of pHLIP, Inc. They have shares in the company, but the company did not fund any part of the work reported in this paper, which was carried out in their academic laboratories.

Abstract

To advance mechanistic understanding of membrane-associated peptide folding and insertion, we have studied the kinetics of three single tryptophan pHLIP (pH-Low Insertion Peptide) variants, where tryptophan residues are located near the N terminus, near the middle, and near the inserting C-terminal end of the pHLIP transmembrane helix. Single-tryptophan pHLIP variants allowed us probing different parts of the peptide in the pathways of peptide insertion into the lipid bilayer (triggered by a pH drop) and peptide exit from the bilayer (triggered by a rise in pH). By using pH jumps of different magnitudes, we slowed down the processes, and established the intermediates that helped us to understand the principles of insertion and exit. The obtained results should also aid the applications in medicine that are now entering the clinic.

Significance

The process of peptide insertion across a membrane is of fundamental interest. It also illuminates our thinking about the ways that lipid boundaries can interact with the molecules they encounter. Obtained in this study results, combined with our recent constant-pH molecular dynamics simulations and kinetics experiments with liposomes of different bilayer thicknesses allowed us to complete a generalized model of the insertion and folding of polypeptides of the pHLIP family, and expand the general view of peptide conformations and dynamic excursions of the bilayer that can accompany interactions with peptides. While the insertion of pHLIPs across membrane bilayers has basic scientific interest, the possibility of clinical applications for tumor imaging and therapy is also emerging as a reality. By understanding the principles of pHLIP properties, the future applications can be broadened and improved.

Introduction

pH-Low Insertion Peptides (pHLIPs®[1]) are being increasingly studied to gain insights concerning peptide folding and insertion into membranes, and to apply them in medicine.

[1] pHLIP® is a registered trademark owned by the Rhode Island Board of Education

Because their membrane insertion from a water-soluble state is triggered by pH changes, a rich opportunity is created for chemical, kinetic and computational studies, as shown by the expanding literature from a growing number of laboratories and ongoing efforts to use them as medically useful acidity sensors *in vivo*. Currently, pHLIPs are being used in studies of membrane-associated folding and unfolding as a model system (1-10), and in a variety of biomedical applications for targeted delivery of imaging and therapeutic agents (11-14). In this paper, we position Tryptophans (Trp) as sensors in the flanking and central regions of a pHLIP and exploit kinetic analysis to study the pathways of membrane entry and exit.

Metabolically active cells, like cancer cells and tumor-associated macrophages within tumors, or activated macrophages in inflamed tissues, are known to acidify their environments (15-18). The extracellular pH in the vicinity of cells in normal healthy tissue is about 7.2-7.4, while pH at the surface of cancer cells could be as low as pH 6.0 (19). Acidity is a possible biomarker for specific targeting of these cells in diseased tissues, but the extracellular pH is only about one pH unit lower than the extracellular pH in healthy organs, creating a challenge for pH-sensitive agents to discriminate between them. A family of pHLIPs was designed to have a variety of properties while sharing the characteristic pHLIP insertion into membrane lipid bilayers at low pHs (<pH7.0) (11, 20, 21). A pHLIP's affinity for a membrane leads to a reversible membrane-adsorbed surface state at high and neutral pHs, which allows a pHLIP to sense the pH at the surfaces of cells (1), triggering insertion if the pH is low. Weak surface binding is useful for a pH-sensing agent, since the pH at the surfaces of cancer cells is 0.5-0.7 pH units lower than the bulk extracellular pH and independent of tumor (tissue) perfusion (19, 22). Another feature of the pHLIP delivery system is that these peptides undergo a cooperative coil-helix transition in response to a pH change, and the pK and cooperativity of the transition are tunable by sequence variation. Further, the activation barrier for insertion into bilayers can be adjusted, pre-determining the time required for cellular targeting and insertion (2, 5, 23). These parameters have utility for pHLIP applications to real biological systems.

To advance understanding of the mechanism of the membrane-associated pHLIP folding we have extended our kinetics studies of single-Trp pHLIP variants. Observations using single-Trp variants have allowed us to observe intermediate steps in the pathways of peptide insertion

into the lipid bilayer triggered by a pH drop and the peptide exit from the bilayer triggered by a rise in pH.

Materials and Methods

pHLIP variants were synthesized and purified by CS Bio Co, and tested for purity by HPLC upon receipt. Small unilamellar vesicles were prepared by extrusion. Steady-state fluorescence and circular dichroism (CD) measurements were performed using a PC1 spectrofluorometer (ISS, Inc) and a MOS-450 spectrometer (Biologic, Inc.), respectively, with temperature control set to 25.0°C. Oriented CD (OCD) measurements were conducted on the supported bilayers placed on quartz slides using the Langmuir-Blodgett system (KSV Nima) as described previously (3). Tryptophan fluorescence and CD kinetics were measured using an SFM-300 mixing system (Bio-Logic Science Instruments) connected to the MOS-450 spectrometer with temperature control set to 25.0°C. All data were fit to the appropriate equations by nonlinear least squares curve fitting procedures employing the Levenberg Marquardt algorithm using Origin 8.5. Detailed descriptions of all methods are presented in the Supporting Information.

Results

We studied the kinetics of insertion into and exit from the lipid bilayer of POPC liposomes using three single Trp pHLIP variants, with the Trp reporters positioned in each flanking region and in the membrane inserted region. pHLIP peptides with a single tryptophan residue allow a “clean” photophysical signals originating from single fluorophores, avoiding spectral heterogeneity. pHLIP variants were designed based on the closely related group of the WT sequences (24), which contains several protonatable residues at the membrane inserting C-terminal end of the peptide. As we demonstrated previously, the presence of protonatable groups at the C-terminus of the peptide slows down the process of insertion of the peptide across a lipid bilayer, as well as slowing exit from the membrane (2, 3). These processes are completed within seconds, as opposed to milliseconds for truncated pHLIPs (2), which allows resolution of structural details along the insertion and exit pathways. The following single Trp pHLIP variants were designed and used in the current study:

pHLIP-W6: ADNNPWIYARYADLTTFPLLLLDLALLVDFDD

pHILP-W17: ADNNPFIYARYADLTTWPLLLLDLALLVDFDD

pHLIP-W30: ADNNPFIYARYADLTTFPLLLLDLALLVDWDD

The length of the designed variants is 32 residues and Trp residues are placed at positions 6, 17 and 30 in the pHLIP sequence in order to be located at the beginning, middle and end of the peptide in its helical inserted form. Phe was replacing other two Trp residues in each variant, which considered to be the best possible substitution of Trp. Using these designs, we can monitor the propagation of different parts of the peptide into and out of the bilayer by recording the changes of their fluorescence signals within single-Trp pHLIP variants.

First, we perfromed equllibrium measurements presented in Figures 1 and 2. Steady-state fluorescence, CD and OCD measurements were used to ensure that each variant is responsive to pH and adopts a TM helical orientation in a POPC bilayer at low pH, which is the main feature of the peptides of pHLIP family (Supplementary Figure S1). Fluorescence spectra were analyzed using the Protein Fluorescence and Structural Tool Kit (PFAST) to determine the positions of spectral maxima (λ_{max}) (25, 26). The transition from the membrane-adsorbed state at high pH to the membrane-inserted state at low pH was assessed from changes of the position of the Trp fluorescence maximum and the ellipticity measured at 222 nm in response to a pH drop from 8.5 to 4 (Figure 1 and Table 1). Analysis of Trp fluorescence reveals the presence of two transitions, which are especially noticeable for the W6 pHLIP variant. The mid-points of the first transition for all variants are established to be around pH 6 with high cooperativity (parameter *n* is from the equation given in the Supplementary Methods section), ranging from 2.4 to 3.5 for different pHLIPs. The second transition is found to be around pH 7.2 with a cooperativity of ranging from 0.5 to 1.6. Interestingly, the CD data reporting the coil-helix transformation are clearly indicative of a single transition with its midpoint at pH 5.8-5.9 and cooperativity ranging from 1.8 to 2.4 for the different pHLIP variants. Note that the transition midpoint is a relatively well defined and stable parameter, while the measured cooperativity is less well determined and might vary over a relatively wide range within experimental error.

The local changes reported by the Trp locations and the general peptide changes reported by CD might be expected to vary from each other, since these parameters might reflect different processes. The high pH transition observed in the fluorescence signal reflects the protonation-deprotonation event, which might be associated with partitioning of regions of the peptide into the lipid bilayer, but not directly associated with the coil-helix transition. The most significant differences occur at the N-terminal part of the pHLIP peptide.

To gain more insight into the locations of Trp residues at different pHs, we carried out Trp fluorescence quenching measurements (Figure 2 and Table 1). The emission of Trp residues was measured at different pHs at increasing concentrations of acrylamide, which is an effective quencher of Trp fluorescence. PFAST analysis was used to calculate Stern-Volmer constants (25, 26) and to calculate the percentage of quenching. At pH 8 and pH 5 the Stern-Volmer plots for all peptide variants demonstrate linear behavior with some upward curvature (Figure 2A and 2D). The upward curvature in quenching by acrylamide was observed before and attributed to the exponential distance-dependent rate of quenching (27). At intermediate pH of 6 a deviation from linearity is observed (Figure 2C), potentially reflecting the existence of different populations of pHLIPs, where Trp residues are located in different environments and their emission is quenched differently by acrylamide (28). Figure 2E and Table 1 reflect gradual decreases of acrylamide quenching of Trp fluorescence with decreases of pH, which can be attributed to the partitioning of Trp residues into the membrane at lower pH and reduction of accessibility to the quencher. The smallest quenching among all pHLIP variants at low pH was observed for the W6 pHLIP variant, reflecting a more solvent-exposed position for Trp6, which correlates well with its higher long-wavelength emission at low pH compared to Trp17 and Trp30.

Insertion and exit kinetics measurements were triggered by a pH drop from 8 to 4 and a pH raise from 4 to 8, respectively (Supplementary Figure S2). Prior to the pH shift, peptide (14 μM) and POPC (2.8 mM) samples were incubated for 24 hrs to reach equilibrium, when most of the peptide is associated with the liposomes (1). As we found previously, the peptide exit from the membrane is much faster than the insertion into the membrane (2, 3). All (or most) protonatable residues in the TM part and at the inserting end of the peptide need to be protonated and became neutral to enter the lipid bilayer, which takes time. On the other hand,

the de-protonation of Asp13 may be enough to induce helix destabilization and peptide exit (4), especially when the C-terminal end of the inserted peptide is in its neutral state due to the fast equilibration of the pH established between the exterior and interior of the liposomes after the pH drop (2). Some differences were observed between variants for the insertion and exit kinetics.

To slow down the kinetic processes and enhance the observed differences we also used intermediate pH jumps: from pH 8 to 5.9-6.2 and from pH 4 to 5.8-6.2, monitoring changes of the fluorescence intensity and the position of maxima of fluorescence spectra during peptide insertion and exit. The changes of fluorescence were recorded at different wavelengths in a global mode, and fluorescence spectra were restored by data processing (Supplementary Figure S3 presents data obtained for Trp30 as an example). Changes of Trp emission intensity recorded at different intermediate pH jumps are shown on Figure 3.

The rates of peptide insertion decrease with decreases of the magnitudes of the pH jumps, and the differences in kinetics pathways between variants become more pronounced (Figure 3 A-C). Trp6 exhibits insertion kinetics with a reversal “kink” where the fluorescence signal first increases, then decays around 15-20 sec after the initiation and is then followed by an emission increase (Figure 3A and 4A). Trp17 reaches its final destination in the membrane rather quickly (Figure 3B). The insertion of Trp30 into the membrane occurs on the time scale of Trp6 and Trp17 insertions. The presence of a “kink” for Trp6 was also observed in the kinetics of the CD signal (Figure 4A) and on the graph of the intensity ratio (Figure 4B) from the fluorescence spectra recorded in the global mode. The ratio is a sensitive measure of the shift of the position of the emission maximum of W6 pHLIP variant insertion. A “kink” was also observed for the Trp30 insertion kinetics by monitoring intensity changes (Figure 4C) and using the intensity ratio (Figure 4D). The data clearly indicate that the propagation of pHLIP peptides into the membrane are associated with a series of changes in the microenvironments of the Trp residues.

The most interesting behavior during the exit of pHLIP variants was observed for Trp30 (Figure 3F and Figure 5). The fluorescence intensity first increased, then was followed by signal decay. The time of the increasing signal was shifted from 1.5 sec in the case of pH jump from pH 4 to 5.8 to 0.4 sec in the case of pH jump from pH 4 to 6.2 (with an intermediate time of 0.92

sec - for the pH jump from 4 to 6.0). While the build up, which is completed within <2 sec, is difficult to resolve in the global mode, the overall intensity decay (Figure 5B) correlates with the 333 nm to 351 nm ratio of emission. As with the insertion measurements, the exit kinetics reveal subtle features not previously observed.

Discussion

To gain understanding of how a peptide can enter and leave a lipid bilayer, we used the pH-triggered insetion and exit of three single-Trp pHLIP variants. We would like to outline that the study is a model biophysical and extreme pHs are set to observe completion of the transitions. Previously it was shown direct correlation between biophysical studies, experiments on cells for delivery of cargo molecules by pHLIP and animal studies for targeting of acidic tumors (23, 24). We found a previously unknown transition at high pH values that is especially pronounced for the N-terminal part of pHLIP. The transition correlates with our recent constant-pH molecular dynamics (MD) calculations, which suggest a high flexibility of the N-terminal flanking sequence of pHLIP (4). At different pH values in the range of 8.5 to 6.5, pHLIP can adopt various conformational states at a bilayer surface, as was noticed previously (6, 8). These conformational changes are not associated with helix formation. A further drop of pH induces the familiar bilayer-associated coil-helix transition, leading to the stabilization of the TM helix at low pH. Trp residues at positions 6 and 30 in the pHLIP sequences adopt similar, partially exposed positions within the lipid bilayer at the outer and inner leaflets, respectively, after peptide insertion, while Trp at position 17 is located near the center. Acrylamide quenching of Trp fluorescence confirmed single component emission at high and low pHs, when peptides are predominantly equilibrated in the inserted or bilayer-adsorbed states, but heterogeneity was observed at intermediate pH of 6. By monitoring signals from single-Trp pHLIP variants, we were able to resolve ambiguities created by the interplay of signals from the two Trps in the WT peptide (9).

By using pH jumps of different magnitudes, we found intermediates that help us to better understand the principles of insertion and exit. If the pH jump is large enough, e.g. a change from pH8 to pH4, it can simultaneously protonate all (or most) of the protonatable residues in the membrane inserting part, and the peptide quickly inserts in a TM orientation.

We previously found that truncation of the C-terminal, inserting part of WT pHLIP can enhance the rate of insertion by two orders of magnitude, revealing that protonated but still polar C-terminal carboxyl groups can pose a significant barrier for transit of the C-terminus across the bilayer, but that entry can still proceed on a timescale of seconds (2, 23). However, if the pH jump is to an intermediate value, the concentration of protons in solution is not enough to fully shift the equilibrium toward the protonated form of residues at the C-terminal part of the peptide, and the peptide is trapped into intermediate states. At intermediate pH jumps N- and C-terminal parts of pHLIP alter their positions toward the bilayer center, while Trp17 adopts a position deep within the membrane rather quickly, as would be consistent with a bent but not inserted conformation. The insertion is completed slowly, consistent with a requirement that protonation of most of the Asp/Glu residues is needed for peptide insertion to proceed at a significant rate. As suggested by MD calculations, and as reasonably expected from the progressively lower dielectric environment, the pKa of protonation is shifted toward higher values as Asp, Glu and the C-terminus move deeper into the bilayer (4).

As previously reported, the exit pathway resulting from a pH raise is different from the pathway of insertion (3). Changes in emission of tryptophan at the C-terminal part of pHLIP sequence (Trp30) during exit add to our understanding of the process, in which an increase of pH leads to the de-protonation of key Asp residues, destabilizing the bilayer-inserted state, and triggering peptide exit. We observed an increase or “build up” of the fluorescence signal, followed by its decay, which clearly documents the exposure of Trp30 to the non-polar bilayer environment along the pathway of peptide exit from the bilayer. The propagation of the C-terminal part of pHLIP through the membrane slows down with a decrease of the magnitudes of the pH jumps.

We believe that our kinetics study, together with recent kinetics experiments on liposomes of different thickness of bilayer (5), theoretical (29) and computational (4) work, frames an improved understanding of the mechanism of pHLIP peptide insertion and exit from a bilayer in response to pH jumps. Figure 6 represents the general scheme of the processes as we now understand it. The membrane-adsorbed state is defined as predominantly unstructured (extended coil) with the C-terminus facing to the outside of a liposome (or extracellular space). The exact position of the peptide at the surface of the bilayer at high and

neutral pH depends on the pHLIP sequence and lipid composition (6, 7, 24, 30). The inserted state is characterized by a transmembrane orientation of the peptide, with the C-terminal end of the peptide facing the liposome interior (or intracellular space). The transition from membrane-adsorbed to inserted states is triggered by pH, which leads to the protonation of at least some Asp and Glu residues, increase of peptide hydrophobicity, deeper partition into bilayer associated with coli-helix transition. We now recognize a set of possible intermediate states, characterized by partially folded structures at the bilayer surface, where the C-terminus is not translocated across the bilayer. The number and nature (transient, semi-stable or stable) of intermediate states is dependent on the number of protonatable groups or polar (charged) cargoes located at the peptide inserting end (2). Charged (or polar) residues and cargoes create forces directed away from the bilayer, which reduces the rate of peptide insertion. As we proposed (2) and recently verified (5), the predominant driving force for the transition from the helical surface intermediate state to the stable membrane inserted state is a relaxation of the membrane distortion created by the inclusion of helical structure at the bilayer surface. The presence of helical instability around the Pro residue in the middle of the helix provides additional flexibility to complete the transition toward a TM orientation. Figure 6 is not a simplified two-state model, it is a generalized model to include the behaviors of various pHLIP sequences within membranes of different lipid compositions.

Recently, a multistage model of WT-pHLIP insertion with distinct equilibrium thermodynamic intermediates has been proposed (8). While it is interesting to think there is a linear progression of states, the fact is that an ensemble of all peptide states exists at each pH, so it remains challenging to define a unique succession. At high and low pH values the predominant, but still not unique states are the peptide membrane-adsorbed and membrane-inserted states, respectively, each of which has a variety of dynamic excursions. However, at intermediate pH values a more distributed mixture of states is present as can be seen in the kinetics measurements, and complexity is shown by the reversal of the fluorescence signal. Of course, in a biological system of living cells in diseased tissues, pH gradients exist across cell membranes, with a low pH at the outside surface of a cell and a higher pH in the cytoplasm (31). In a tumor cell , the pH at the cell surface can be below 6 while the pH inside the cell is thought to be around 7.4. The pH gradient tends to stabilize the inserted state, since any C-

terminal protonatable residues translocated across the membrane into the cytoplasm will be relatively de-protonated in the environment of the normal pH of the cytoplasm, which leads to a significant reduction of the rate of peptide exit from the membrane.

Thermodynamics is not limiting for the intracellular delivery of cargo conjugated to pHLIP C-terminal inserting end, since the equilibrium of the pHLIP peptide in a cell with an acidic diseased phenotype will be as a TM helix and the chemical potential of the cargo will be about the same on either side of the membrane. Given enough time for equilibration, even polar or charged cargoes could be delivered into cells and trapped in the cytoplasm. However, in a living biological system the circulatory and other dynamics will tend to remove uninserted pHLIP complexes, so the kinetics of insertion becomes an important factor for tumor targeting and cargo delivery. Since pHLIPs have a significant affinity for bilayer surfaces, they sense the pH at the surfaces of cells in diseased tissues, and when pH is low, pHLIPs insert into cellular membrane. The rate of insertion depends on several factors: i) the level of acidity in the vicinity of cell membrane; ii) number of polar/charged residues at the membrane-inserting end of the peptide and/or polarity/charge of cargo molecule (if any), which peptide is translocating (flipping) across membrane, and iii) composition, thickness and fluidity of membrane (2, 5).

While the insertion of pHLIPs across membrane bilayers is of basic scientific interest, the possibility of clinical applications for tumor imaging and therapy is emerging as a reality. Clinical trials for applications to the targeting of imaging agents are about to start, with the first patients being scheduled at the time of this writing, and trials based on targeting tissues with a therapeutic agent are anticipated in 2020. By understanding the principles of pHLIP properties, it is likely that future applications can be broadened and improved.

References

1. Reshetnyak YK, Andreev OA, Segala M, Markin VS, & Engelman DM (2008) Energetics of peptide (pHLIP) binding to and folding across a lipid bilayer membrane. *Proceedings of the National Academy of Sciences* 105(40):15340-15345.
2. Karabadzhak AG*, et al.* (2012) Modulation of the pHLIP transmembrane helix insertion pathway. *Biophys J* 102(8):1846-1855.
3. Andreev OA*, et al.* (2010) pH (low) insertion peptide (pHLIP) inserts across a lipid bilayer as a helix and exits by a different path. *Proc Natl Acad Sci U S A* 107(9):4081-4086.
4. Vila-Vicosa D*, et al.* (2018) Membrane-Induced p Ka Shifts in wt-pHLIP and Its L16H Variant. *J Chem Theory Comput* 14(6):3289-3297.

5. Karabadzhak AG*, et al.* (2018) Bilayer Thickness and Curvature Influence Binding and Insertion of a pHLIP Peptide. *Biophys J* 114(9):2107-2115.
6. Vasquez-Montes V, Gerhart J, King KE, Thevenin D, & Ladokhin AS (2018) Comparison of lipid-dependent bilayer insertion of pHLIP and its P20G variant. *Biochim Biophys Acta Biomembr* 1860(2):534-543.
7. Kyrychenko A, Vasquez-Montes V, Ulmschneider MB, & Ladokhin AS (2015) Lipid headgroups modulate membrane insertion of pHLIP peptide. *Biophys J* 108(4):791-794.
8. Otieno SA*, et al.* (2018) pH-dependent thermodynamic intermediates of pHLIP membrane insertion determined by solid-state NMR spectroscopy. *Proc Natl Acad Sci U S A* 115(48):12194-12199.
9. Hanz SZ*, et al.* (2016) Protonation-Driven Membrane Insertion of a pH-Low Insertion Peptide. *Angew Chem Int Ed Engl* 55(40):12376-12381.
10. Shu NS, Chung MS, Yao L, An M, & Qiang W (2015) Residue-specific structures and membrane locations of pH-low insertion peptide by solid-state nuclear magnetic resonance. *Nat Commun* 6:7787.
11. Wyatt LC, Lewis JS, Andreev OA, Reshetnyak YK, & Engelman DM (2017) Applications of pHLIP Technology for Cancer Imaging and Therapy. *Trends Biotechnol* 35(7):653-664.
12. Bernardo BC, Ooi JY, Lin RC, & McMullen JR (2015) miRNA therapeutics: a new class of drugs with potential therapeutic applications in the heart. *Future Med Chem* 7(13):1771-1792.
13. Andreev OA, Engelman DM, & Reshetnyak YK (2014) Targeting diseased tissues by pHLIP insertion at low cell surface pH. *Front Physiol* 5:97.
14. Pereira MC, Reshetnyak YK, & Andreev OA (2015) Advanced targeted nanomedicine. *J Biotechnol* 202:88-97.
15. Pillai SR*, et al.* (2019) Causes, consequences, and therapy of tumors acidosis. *Cancer Metastasis Rev* 38(1-2):205-222.
16. Damgaci S*, et al.* (2018) Hypoxia and acidosis: immune suppressors and therapeutic targets. *Immunology* 154(3):354-362.
17. Kato Y*, et al.* (2013) Acidic extracellular microenvironment and cancer. *Cancer Cell Int* 13(1):89.
18. Netea-Maier RT, Smit JWA, & Netea MG (2018) Metabolic changes in tumor cells and tumor-associated macrophages: A mutual relationship. *Cancer Lett* 413:102-109.
19. Anderson M, Moshnikova A, Engelman DM, Reshetnyak YK, & Andreev OA (2016) Probe for the measurement of cell surface pH in vivo and ex vivo. *Proc Natl Acad Sci U S A* 113(29):8177-8181.
20. Andreev OA, Engelman DM, & Reshetnyak YK (2010) pH-sensitive membrane peptides (pHLIPs) as a novel class of delivery agents. *Mol Membr Biol* 27(7):341-352.
21. Andreev OA, Engelman DM, & Reshetnyak YK (2009) Targeting acidic diseased tissue: New technology based on use of the pH (Low) Insertion Peptide (pHLIP). *Chim Oggi* 27(2):34-37.
22. Wei D, Engelman DM, Reshetnyak YK, & Andreev OA (2019) Mapping pH at Cancer Cell Surfaces. *Mol Imaging Biol*.
23. Weerakkody D*, et al.* (2013) Family of pH (low) insertion peptides for tumor targeting. *Proc Natl Acad Sci U S A* 110(15):5834-5839.
24. Wyatt LC*, et al.* (2018) Peptides of pHLIP family for targeted intracellular and extracellular delivery of cargo molecules to tumors. *Proc Natl Acad Sci U S A* 115(12):E2811-E2818.
25. Shen C*, et al.* (2008) The protein fluorescence and structural toolkit: Database and programs for the analysis of protein fluorescence and structural data. *Proteins* 71(4):1744-1754.
26. Burstein EA, Abornev SM, & Reshetnyak YK (2001) Decomposition of protein tryptophan fluorescence spectra into log-normal components. I. Decomposition algorithms. *Biophys J* 81(3):1699-1709.

27. Zelent B, Kusba J, Gryczynski I, Johnson ML, & Lakowicz JR (1993) Distance-dependent fluorescence quenching ofN-acetyl-L-tryptophanamide by acrylamide. *J Fluoresc* 3(3):199-207.
28. Reshetnyak YK & Burstein EA (2001) Decomposition of protein tryptophan fluorescence spectra into log-normal components. II. The statistical proof of discreteness of tryptophan classes in proteins. *Biophys J* 81(3):1710-1734.
29. Sharma GP, Reshetnyak YK, Andreev OA, Karbach M, & Muller G (2015) Coil-helix transition of polypeptide at water-lipid interface. *J Stat Mech* 2015.
30. Scott HL, Heberle FA, Katsaras J, & Barrera FN (2019) Phosphatidylserine Asymmetry Promotes the Membrane Insertion of a Transmembrane Helix. *Biophys J* 116(8):1495-1506.
31. Swietach P, Vaughan-Jones RD, Harris AL, & Hulikova A (2014) The chemistry, physiology and pathology of pH in cancer. *Philos Trans R Soc Lond B Biol Sci* 369(1638):20130099.

Tables

Table 1. Tryptophan emission parameters obtained from steady-state fluorescence and CD measurements (mean ± standard deviation) are presented. The tryptophan fluorescence spectra were processed by PFAST to identify positions of spectral maxima (λ_{max}). Values of λ_{max} were averaged over several different steady-state fluorescence measurements. The parameters representing transitions induced by a pH drop from 9 to 3, including the midpoint of the pH transition (*pK*) and cooperativity (*n*), were calculated by fitting values of the position of maximum of fluorescence (Fluor) and ellipticity at 222 nm (CD) measured at different pHs. The Stern-Volmer constants (K_{SV}, M^{-1}) for acrylamide quenching of tryptophan fluorescence of peptides in POPC liposomes at different pHs were obtained after PFAST analysis of fluorescence spectra.

	W6	**W17**	**W30**
λ_{max}, pH8 (nm)	349.5 ± 0.4	349.2 ± 0.3	352.1 ± 0.4
λ_{max}, pH8 + PC (nm)	347.9 ± 0.9	346.9 ± 0.8	350.4 ± 0.3
λ_{max}, pH5 + PC (nm)	340.4 ± 0.7	332.3 ± 1.6	339.7 ± 0.9
Fluor, pK_1	6.0 ± 0.0	6.0 ± 0.0	6.1 (fixed)
Fluor, n_1	3.5 ± 0.3	2.6 ± 0.1	2.4 ± 0.2
Fluor, pK_2	7.2 ± 0.1	7.3 ± 0.1	7.2 (fixed)
Fluor, n_2	1.6 ± 0.4	1.2 ± 0.4	0.5 ± 0.1
CD, *pK*	5.9 ± 0.0	5.8 ± 0.0	5.8 ± 0.0
CD, *n*	2.2 ± 0.2	2.4 ± 0.2	1.8 ± 0.2
K_{sv}, pH7.9-8.1 PC (M^{-1})	20.5 ± 3.5	20.1 ± 2.1	21.2 ± 3.9
K_{sv}, pH7.0-7.3 PC (M^{-1})	19.3 ± 0.5	18.2± 1.1	18.1 ± 0.4
K_{sv}, pH5.9-6.2 PC (M^{-1})	8.0 ± 0.6	11.6 ± 1.7	12.6± 0.7
K_{sv}, pH4.8-5.0 PC (M^{-1})	6.2 ± 0.9	2.4 ± 0.1	2.9 ± 0.2

Figure Legends

Figure 1. pH-dependent bilayer insertion of pHLIP variants. The pH-dependent insertion of W6 (A and D), W17 (B and E) and W30 (C and F) pHLIP variants into the lipid bilayers of POPC liposomes was studied by monitoring the changes in the position of maxima of tryptophan fluorescence spectra (A-C) and ellipticity of CD signals measured at 222 nm (D-F) as function of pH. The data were fitted using the Henderson-Hasselbalch equation, the fitting curves and 95% confidence interval are shown by red and pink areas, respectively.

Figure 2. Acrylamide quenching. Quenching of tryptophan fluorescence of W6, W17 and W30 pHLIP variants in presence of POPC liposomes at the range of pH values: pH7.9-8.1 (A), pH7.0-7.3 (B), pH5.9-6.2 (C), pH4.8-5.0 (D) are presented. The percentage of quenching at different pHs calculated for different pHLIP variants is shown in panel E, assuming quenching of tryptophan in solution by acrylamide (21 M^{-1}) to be 100%.

Figure 3. Kinetics of insertion and exit. Representative kinetic curves for the insertion (A-C) of W6 (A, D), W17 (B, E) and W30 (C, F) pHLIP variants into the lipid bilayer triggered by drops of pH from pH8 to pHs 5.8, 6.0 and 6.2, and for the exit (D-F) of W6 (A, D), W17 (B, E) and W30 (C, F) pHLIP variants out of the lipid bilayer triggered by raises of pH from pH4 to pHs 5.8, 6.0 and 6.2 are shown. The normalized fluorescence measured via 320 cut off filter is presented.

Figure 4. Kinetics of insertion. Representative kinetic curves for the insertion of W6 (A, B) and W30 (C, D) pHLIP variants into the lipid bilayer triggered by drops of pH from pH8 to pH5.8-5.9, and from pH8 to pH6.2, respectively, are shown. The peptides insertion was monitored by changes of fluorescence intensity (A, C) and ratios of fluorescence measured at different wavelengths in the global mode kinetics experiments (B, D). The W6 pHLIP variant folding and unfolding was monitored by changes of the CD signal (A). Red curves in panels B, C and D represent averages of the measured signal shown in black.

Figure 5. Kinetics of exit. Representative kinetic curves for the exit of the W30 pHLIP variant from the lipid bilayer triggered by raises of pH from pH4 to pHs 5.8, 6.0 and 6.2 are shown. The

peptide exit from the membrane was monitored by changes of fluorescence intensity (A, B) and ratio of fluorescence measured at different wavelengths in global mode kinetics experiments (C). Red curve at panel C represents averaged of the measured signal shown in black.

Figure 6. Model of pHLIP insertion and exit. Schematic presentation of pHLIP folding and insertion into a bilayer, as well as the pHLIP exit and unfolding are shown. Approximate locations of Trp6, Trp17 and Trp30 are shown by green, blue and yellow colors, respectively. The structure of WT pHLIP in the membrane-inserted state was taken from the results of MD simulations (15).

Figures

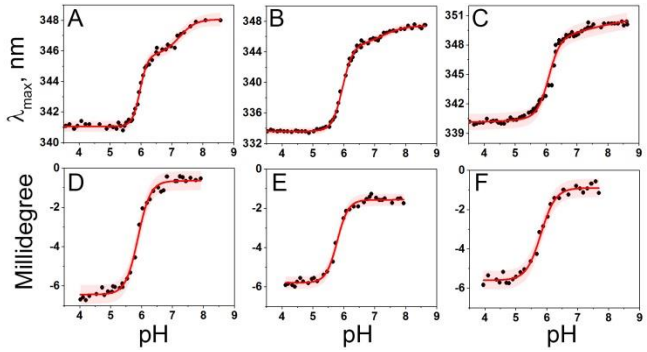

Figure 1

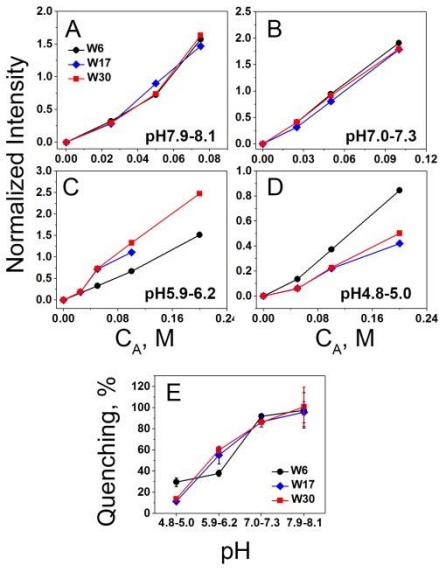
A
W6
W17
W30
pH7.9-8.1
B
pH7.0-7.3
C
pH5.9-6.2
D
pH4.8-5.0
Normalized Intensity
C_A, M
C_A, M
E
Quenching, %
W6
W17
W30
4.8-5.0 5.9-6.2 7.0-7.3 7.9-8.1
pH

Figure 2

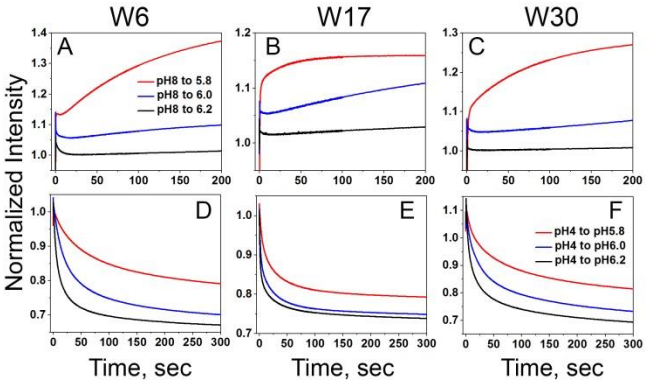
W6
W17
W30
A
B
C
D
E
F
pH8 to 5.8
pH8 to 6.0
pH8 to 6.2
pH4 to pH5.8
pH4 to pH6.0
pH4 to pH6.2
Normalized Intensity
Time, sec
Time, sec
Time, sec

Figure 3

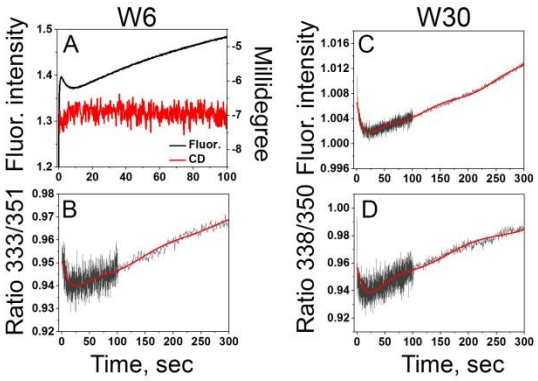
W6
W30
A
B
C
D
Fluor. intensity
Ratio 333/351
Ratio 338/350
Millidegree
Fluor.
CD
Time, sec
Time, sec

Figure 4

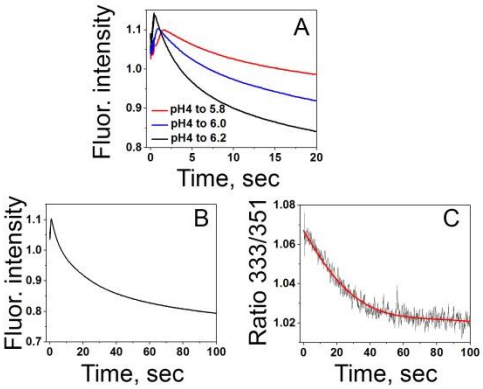
A
Fluor. intensity
pH4 to 5.8
pH4 to 6.0
pH4 to 6.2
Time, sec
B
Fluor. intensity
Time, sec
C
Ratio 333/351
Time, sec

Figure 5

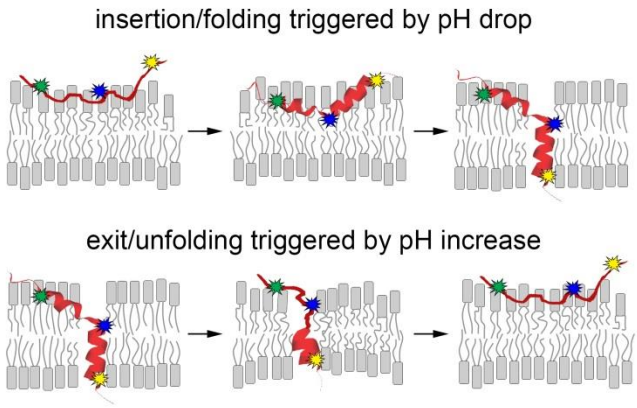
insertion/folding triggered by pH drop
exit/unfolding triggered by pH increase

Figure 6

Supporting Information

Methods

Peptide Preparation

Peptides were synthesized and purified by CSBio (Menlo Park, CA). Purified peptides were dissolved in 6 M urea and passed through a G-10 size exclusion spin column to transfer to 10 mM phosphate buffer, pH 8. Peptide concentrations were calculated using absorbance measurements at 280 nm, where $\varepsilon_{280} = 8{,}520\ M^{-1} \cdot cm^{-1}$.

Liposome Preparations

Small unilamellar vesicles were prepared by extrusion. 1-Palmitoyl-2-oleoyl-sn-glycero-3-phosphocholine (POPC, Avanti Polar Lipids, Inc.) dissolved in chloroform at a concentration of 12.5 mg/ml was desolvated in a rotary evaporator to create a phospholipid film and placed under high vacuum for 2 hours. Lipids were then rehydrated in phosphate buffer (pH 8) and extruded through membranes with pore size of 50 nm. The liposome size distribution was measured using a nanoparticle tracking system, Nanosight (NS300, Malvern).

Equillibrium Measurements

Steady-State fluorescence and CD

All steady-state spectral measurments including fluorescence, circular dichroism (CD), oriented CD (OCD), pH-dependence and acrylamide quenching were performed using a PC1 spectrofluorometer (ISS, Inc) and a MOS-450 spectrometer (Biologic, Inc with temperature control set to 25.0°C. Tryptophan fluorescence spectra were recorded from 310 to 390 nm with step of 1 or 2 nm using an excitation wavelength of 295 nm. Excitation and emission polarizers were set to 54.7° and 0.0°, respectively. CD and OCD spectra were recorded from 195 to 260 nm with step of 1 nm. The concentration of peptide and liposomes were 7 μM and 1.4 mM, respectively.

Oriented CD

OCD measurements were conducted on supported bilayers deposited on quartz slides using a Langmuir-Blodgett system (KSV Nima). Fourteen slides were cleaned using the following protocol; sonication for 10 min in cuvette cleaner solution (5% Contrad in water), 2-propanol, acetone, 2-propanol, followed by rinsing in deionized water. Finally, the slides were immersed in a mixture of concentrated sulfuric acid and hydrogen peroxide (3:1 ratio) for 5 min to remove any remaining organic material and then rinsed three times in deionized water. The slides were stored in deionized water until the monolayers were applied. The POPC monolayers were deposited on the quartz slides using a KSV minitrough. For the Langmuir-Blodgett system, POPC dissolved in chloroform solution at 3 mg/ml was spread on subphase. After allowing chloroform to evaporate, the POPC monolayer was compressed to 32 mN/m. The initial layers on the slides were deposited by retrieving the slide from the subphase at a rate of 15 mm/min, and the second layer was added by introducing a solution of 10 μM peptide and 1 mM POPC liposomes (50-nm in size) at pH 4, resulting in the creation of the supported bilayer via fusion of one layer with liposomes. After incubation for 6 h at 100% humidity, excess vesicles were carefully removed, buffer at pH 4 was added to the spaces between slides, and the slides were stacked with 0.2-mm spacers. CD measurements were taken at three time points: immediately after the

addition of the peptide/liposome solution (0 h), after 6 h and 12 h of incubation time (6 h and 12 h).

pH dependence

The pH-dependent insertion of the peptides into the lipid bilayer of liposomes was studied by monitoring either the changes in tryptophan fluorescence spectra or changes in the molar ellipticity at 222 nm as a function of pH. After the addition of aliquots of citric acid, the pHs of solutions containing 7 µM peptide and 1.4 mM POPC liposomes were measured using an Orion PerHecT ROSS Combination pH Micro Electrode and an Orion Dual Star pH and ISE Benchtop Meter before and after each spectrum measurement to ensure that equilibrium is achieved. The tryptophan fluorescence at each pH was measured on a PC1 spectrofluorometer. Fluorescence spectra were analyzed using the Protein Fluorescence and Structural Tool Kit (PFAST) to determine the positions of spectral maxima (λ_{max}). Finally, λ_{max} or millidegree were plotted as a function of pH. The pH-dependence was fit with the Henderson-Hasselbach equation (using OriginLab software) to determine the cooperativity (n_i) and the mid-point (pK) of a single or two transitions: $Normalized\ pH\ dependence = \frac{1}{1+10^{n_i(pH-pK_i)}}$

Acrylamide quenching

Tryptophan fluorescence quenching experiments were conducted using acrylamide in the cuvette of 3 x 3 mm. Solutions containing 7 µM of pHLIP peptides and 1.4 mM of POPC liposomes were adjusted to about pH 8, 7, 6, or 5. Tryptophan fluorescence quenching was achieved by addition of increasing amounts of acrylamide. Different amounts of acrylamide used for different pH values (the maximum was 0.2-0.3 M of acrylamide for measurements performed at low pH). The obtained data were corrected for the dilution and inner filter effect taking into account that the exctiction coefficient for acrylamide at 295 nm is 0.25 $M^{-1}cm^{-1}$. PFAST analysis was employed to calculate Stern-Volmer constants and to calculate the percentage of quenching (100% was assigned to the quenching of tryptophan in solution, K_{SV} = 21 M^{-1}).

Kinetics Measurements

Tryptophan fluorescence and CD kinetics were measured using a SFM-300 mixing system (Bio-Logic Science Instruments) in combination with the MOS-450 spectrometer with temperature control set to 25.0°C. All samples were degassed before measurements to minimize air bubbles in the samples. Peptide (14 µM) and POPC (2.8 mM) samples were incubated for 24 hrs to reach equilibrium, when most of the peptide is associated with liposome lipid bilayers. To follow peptide insertion, equal volumes of peptide-POPC solution and citric acid were fast mixed (5-ms dead time) to lower the pH from pH 8 to the desired lower pH value. To measure peptide exit, equal volumes of peptide-POPC solution and disodium phosphate were mixed to raise the pH from pH 4 to the desired higher pH value. To monitor fluorescence intensity changes during peptide insertion or exit, the tryptophan emission signal was observed through a cut off 320 nm filter at an excitation of 295 nm. To monitor the shift of the entire tryptophan spectra of the peptides during insertion and exit, (excited at 295 nm) an emission monochromator was used. In the latter case, fluorescence kinetics spectra were recorded in a global mode at individual emission wavelengths from 321 nm to 366 nm with steps of 3 nm. Three-dimensional plots were constructed reflecting changes in fluorescence intensity, time, and wavelength. Two-

dimensional plots were made by taking cross sections at particular times and plotting intensity vs. wavelength. To monitor coil-helix transition (and vice versa) the CD signal at 222 nm was recorded.

Data analysis

All data were fit to the appropriate equations by nonlinear least squares curve fitting procedures employing the Levenberg Marquardt algorithm using Origin 8.5.

Figures

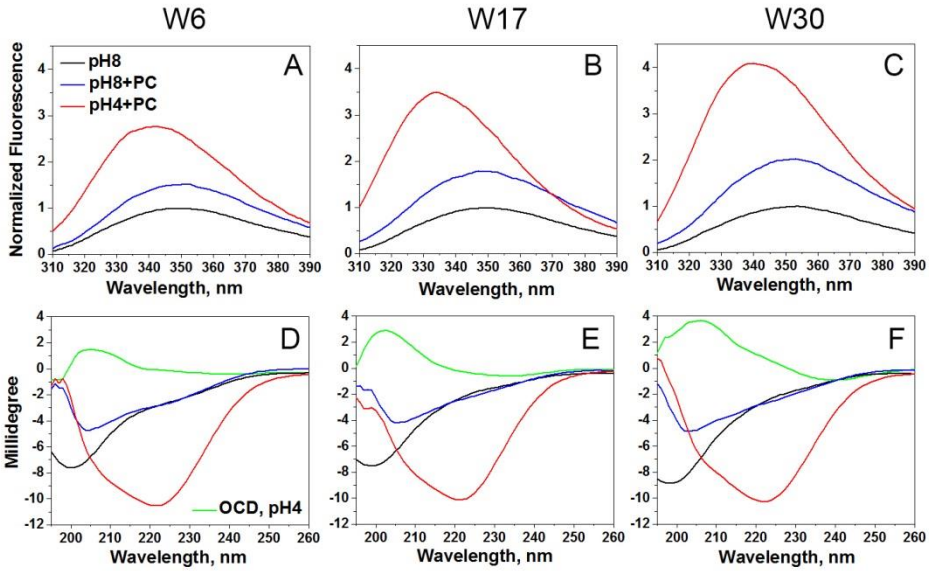

Figure S1. Tryptophan fluorescence (A-C), CD and OCD (D-F) spectra are shown from Trp6 (A, D), Trp17 (B, E) and Trp30 (C, F) pHLIP variants: in aqueous solution at pH 8 (black lines), at pH8 in the presence of POPC liposomes (blue lines) and at pH4 in the presence of POPC liposomes (red lines). Oriented circular dichroism (OCD) signals measured at low pH in supported bilayers are shown in panels D-F (green curves).

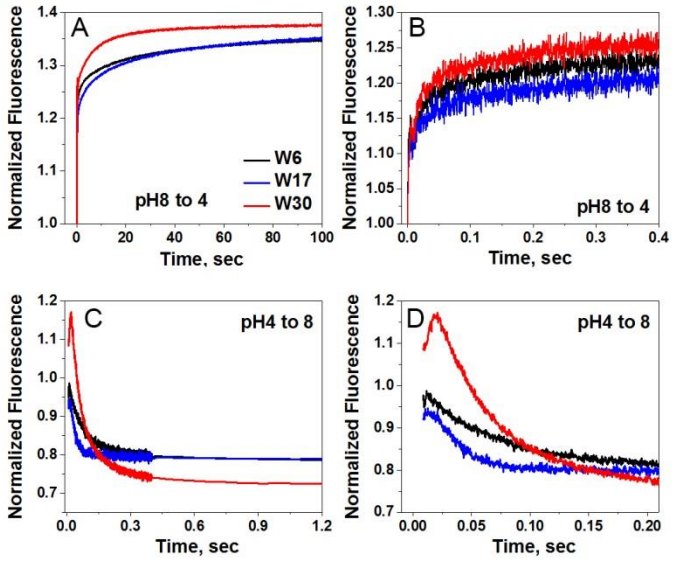

Figure S2. Trp fluorescence kinetics measurements of pHLIP peptide insertion and exit are shown over different time scales for Trp6 (black lines), Trp17 (blue lines), and Trp30 (red lines) pHLIP variants. Insertion is triggered by a pH jump from pH8 to pH4 (A, B) and exit by a pH jump from pH4 to pH8 (C, D).

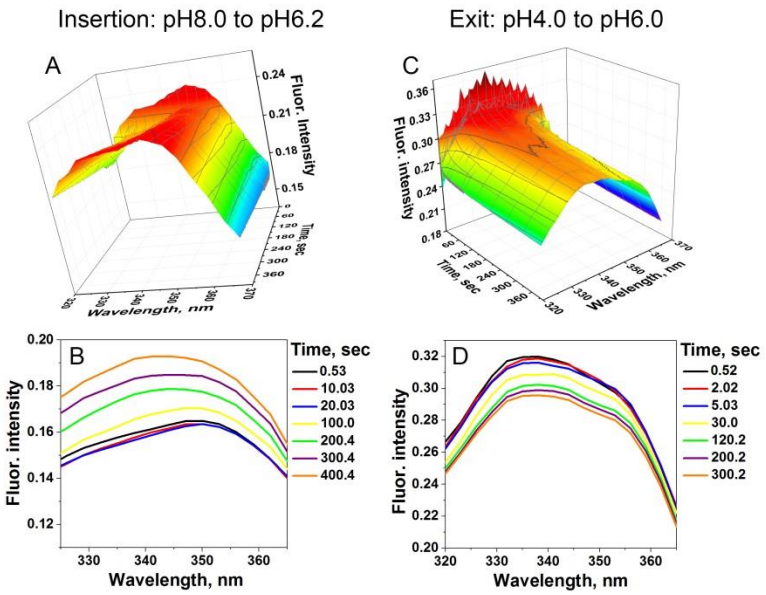

Figure S3. 3D (A, C) and 2D (B, D) representations are shown for the insertion (A, B) and exit (C, D) kinetics of Trp30, on the inserting C-terminal flank of the pHLIP peptide. Spectral regions of the fluorescence reveal complex pathways, as in the short wavelengths for insertion seen in A. The 3D plots (A, C) reflect changes in fluorescence intensity, time, and wavelength (the axis are the same on both panels, but angle views are different for better presentation). The 2D plots (B, D) show cross sections of the 3D plots at selected time points.